Energy Conversion and Management 274 (2022) 116458

Contents lists available at ScienceDirect

Energy Conversion and Management

journal homepage: www.elsevier.com/locate/enconman

Blue, green, and turquoise pathways for minimizing hydrogen production costs from steam methane reforming with CO_2 capture

Florian Pruvost [a], Schalk Cloete [b], Carlos Arnaiz del Pozo [c], Abdelghafour Zaabout [b,*]

[a] Génie Chimique, Toulouse INP-ENSIACET, Toulouse, France
[b] Process Technology Department, SINTEF Industry, Trondheim, Norway
[c] Departamento de Ingeniería Energética, Universidad de Politécnica de Madrid, Madrid, Spain

ARTICLE INFO

Keywords:
Hydrogen production
Steam methane reforming
CO_2 capture
Methane pyrolysis
Techno-economic assessment

ABSTRACT

Rising climate change ambitions require large-scale clean hydrogen production in the near term. "Blue" hydrogen from conventional steam methane reforming (SMR) with pre-combustion CO_2 capture can fulfil this role. This study therefore presents techno-economic assessments of a range of SMR process configurations to minimize hydrogen production costs. Results showed that pre-combustion capture can avoid up to 80% of CO_2 emissions cheaply at 35 €/ton, but the final 20% of CO_2 capture is much more expensive at a marginal CO_2 avoidance cost around 150 €/ton. Thus, post-combustion CO_2 capture should be a better solution for avoiding the final 20% of CO_2. Furthermore, an advanced heat integration scheme that recovers most of the steam condensation enthalpy before the CO_2 capture unit can reduce hydrogen production costs by about 6%. Two hybrid hydrogen production options were also assessed. First, a "blue-green" hydrogen plant that uses clean electricity to heat the reformer achieved similar hydrogen production costs to the pure blue configuration. Second, a "blue-turquoise" configuration that replaces the pre-reformer with molten salt pyrolysis for converting higher hydrocarbons to a pure carbon product can significantly reduce costs if carbon has a similar value to hydrogen. In conclusion, conventional pre-combustion CO_2 capture from SMR is confirmed as a good solution for kickstarting the hydrogen economy, and it can be tailored to various market conditions with respect to CO_2, electricity, and pure carbon prices.

Acronyms

ACF	Annualized cash flow rate
BEC	Bare erected cost
CAC	CO_2 avoidance cost
CCS	Carbon capture and storage
EPC	Engineering, procurement and construction
FOM	Fixed operating and maintenance
FTR	Fired tubular reformer
HP	High pressure
HTS	High temperature shift
LCOH	Levelized cost of hydrogen
LHV	Lower heating value
LP	Low pressure
LTS	Low temperature shift
MDEA	Methyl-diethanolamine
NG	Natural gas
NPV	Net present value
OC	Owner's costs
PC	Project contingency
PSA	Pressure swing adsorption
SMR	Steam methane reforming
SEA	Standardised economic assessment
S/C	Steam to carbon
TOC	Total overnight costs
VOM	Variable operating and maintenance
WGS	Water-gas shift

List of symbols

C_{CO_2}	Carbon capture rate (%)
E_{CO_2}	Specific emissions (kg/kg)
P_{H_2}	Yearly hydrogen production (kg/year)
M_r	Molecular weight (kg/kmol)
i	Discount rate (%)

* Corresponding author at: Flow Technology Group, SINTEF Industry, S.P. Andersens vei 15 B, 7031 Trondheim, Norway.
E-mail address: abdelghafour.zaabout@sintef.no (A. Zaabout).

https://doi.org/10.1016/j.enconman.2022.116458
Received 1 June 2022; Received in revised form 30 October 2022; Accepted 3 November 2022
Available online 18 November 2022

n	Plant lifetime (years)
η	Efficiency (%)
ϕ	Capacity factor (%)
$\dot{m}$	Flow rate (kg/s)
$\dot{W}$	Power (kW)

1. Introduction

After decades of little progress, there is finally some real momentum behind the well-established idea of a hydrogen economy. In addition to a dedicated hydrogen report by the International Energy Agency [1], several governments and industry groups have compiled ambitious near-term hydrogen strategies [2–6]. Thus, there is an urgent need for deployment of low-carbon hydrogen production facilities.

The two foremost technologies for producing low-carbon hydrogen in the near term are steam methane reforming (SMR) with conventional CO_2 capture technology (blue hydrogen) and water electrolysis using renewable electricity (green hydrogen). Today, SMR without CO_2 capture (grey hydrogen) provides the bulk of global hydrogen production because avoiding CO_2 emissions is expensive and technically challenging. For blue hydrogen, CO_2 capture introduces additional costs and large-scale infrastructure for CO_2 transport and storage is not yet widely available. Furthermore, CO_2 capture using conventional technologies is incomplete, implying the blue hydrogen still involves significant CO_2 emissions. Electrolysers for green hydrogen production are still expensive and electricity in most world regions remains relatively carbon intensive. Producing pure green hydrogen from dedicated wind and solar installations involves substantial under-utilization of the electrolyser capacity and introduces challenges with handling the intermittent fluxes of hydrogen output, both leading to substantial added costs [7].

In the long term, both blue and green hydrogen is expected to become substantially cheaper. For blue hydrogen, several advanced process routes are being investigated, including chemical looping reforming [8], gas switching reforming in packed [9] and fluidized [10] beds, membrane-assisted chemical looping [11] and autothermal [12] reforming, and sorbent-enhanced SMR [13]. All these concepts can substantially reduce the costs of CO_2 capture leading to very low [14] or even negative [11] CO_2 avoidance costs, while achieving near-complete CO_2 capture. Furthermore, falling fossil fuel demand in the future may reduce natural gas prices (usually the largest cost component of blue hydrogen). For example, European natural gas prices in the International Energy Agency's Sustainable Development Scenario [15] are projected to decline by almost 30 % by 2025 from 2019 levels. Green hydrogen is expected to achieve even more dramatic cost reductions due to declining investment costs of electrolysers and renewable electricity [16]. It can also play an important role in integrating higher shares of wind and solar power by concentrating production during times of excess electricity production, although this benefit is counteracted by low capital utilization of electrolysers and downstream hydrogen compression, transmission, and storage infrastructure.

Ultimately, it is likely that both blue and green hydrogen will be required in the global decarbonization effort. Natural gas and wind/solar resources vary greatly across the world and hydrogen is challenging and expensive to trade internationally [1]. Therefore, the cost of locally available input energy is likely to dictate the relative competitiveness of blue and green hydrogen, securing a place for both in the global energy mix of the future. However, successful near-term deployment of low-carbon hydrogen production facilities is vital to kickstart the hydrogen economy by stimulating the creation of additional hydrogen demand and the wide range of infrastructure linking supply and demand.

In light of the urgent need for cost-effective near-term clean hydrogen production, the present study seeks to maximize the potential of blue hydrogen production using the conventional SMR route with pre-combustion CO_2 capture. Although CO_2 can be captured at different locations in the SMR process (Fig. 1), removal before the pressure swing adsorption (PSA) unit is most cost effective [17] due to the high CO_2 partial pressure in the pressurized syngas stream and decreased volumetric flow rate through the PSA after CO_2 separation. The drawback of this route is that a considerable amount of carbon as unconverted CH_4 and CO passes through this CO_2 capture step to be combusted as PSA off-gas fuel in the reformer furnace with the resulting CO_2 being emitted to the atmosphere. In fact, only about 56 % of CO_2 is captured when conventional steam-to-carbon (S/C) ratios with only a high-temperature water–gas shift (WGS) step are used [17]. An S/C ratio of 4 with the inclusion of low-temperature WGS can raise the CO_2 capture ratio to 85 % by converting additional CH_4 and CO to CO_2 and H_2, albeit at a considerable energy penalty [13].

It is generally assumed that post-combustion CO_2 capture is required for high CO_2 capture ratios, but this route is relatively costly because the CO_2 partial pressure in the flue gas is more than an order of magnitude lower than in the pressurized syngas before the PSA. However, there is a route for reaching very high CO_2 capture ratios via pre-combustion capture that has not yet been well explored in the literature: PSA off-gas recycling. In this configuration, most of the PSA off-gas is mixed with the natural gas feed to the reformer and most of the reforming heat supplied by combusting some of the hydrogen product. Such an arrangement also lends itself well to the concept of electrified reforming [18] where ohmic heating is used to drive the endothermic reforming reactions instead of combusting some of the valuable hydrogen product. The potential of these solutions for improved CO_2 capture ratios can be further enhanced by advanced heat integration and pre-reforming strategies.

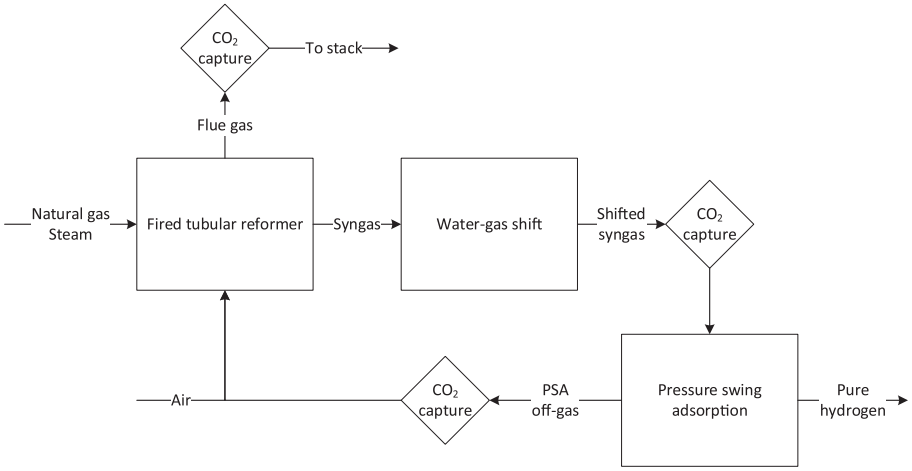

Fig. 1. Simplified block diagram indicating the three possible locations for CO_2 capture in an SMR plant.

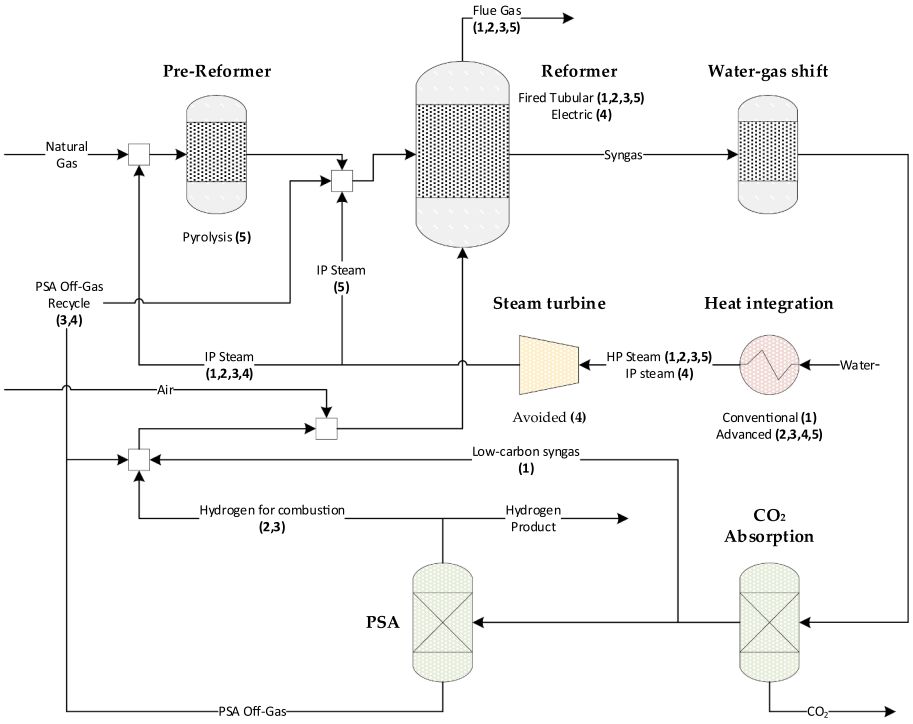

Fig. 2. Simplified layout explaining the five cases considered in the present study. The areas where the cases differ are indicated by numbers: 1) Base case, 2) Advanced heat integration, 3) Recycling for higher CO_2 capture, 4) Ohmic reformer heating, 5) Pyrolysis for higher hydrocarbon cracking. A detailed flowsheet with stream data for each case is available in the Supplementary Material.

In light of these opportunities, the present study makes the following novel contributions to the scientific literature: 1) quantification of the marginal costs of increasing CO_2 avoidance from pre-combustion CO_2 capture via higher steam-to-carbon and PSA off-gas recycle ratios, 2) quantification of the potential of advanced heat integration strategies to enhance efficiency and reduce costs, 3) a consistent benchmarking of electrified reforming against the reference process and quantification of its potential to contribute to balancing wind and solar power, and 4) quantification of the economic benefits of a new pre-reforming strategy using molten salt pyrolysis.

2. Methodology

In this section, a detailed description of the conventional SMR plant with pre-combustion CO_2 capture using Methyl-diethanolamine (MDEA) absorption is provided. Subsequently, the different plant enhancements from an energetic and environmental perspective are presented. Finally, plant performance indicators from an energy, environmental and economic perspective are defined, while the main economic assumptions employed are provided. Simulations were carried out in Aspen Plus V10. The Peng-Robinson equation of state is employed for property estimation. Both in the reformer (including the combustion furnace) and the WGS units, reactions are assumed to proceed to equilibrium. Further modelling assumptions are provided in the Supplementary Information attached to this manuscript.

2.1. SMR with CCS

The standard SMR plant with pre-combustion CO_2 capture by means of MDEA absorption is based on the configuration presented in previous literature studies [11,13,17]. Assumptions regarding equilibrium conditions in the reforming and shift reactors at the temperatures and pressures outlined below are well established in these studies, including one from an SMR technology supplier [17], providing a realistic representation of the performance of real-world SMR plants. The performance assumptions of pre-combustion CO_2 capture using MDEA from these studies are similarly well established, also agreeing with more detailed modelling studies of this unit [19].

The natural gas feed is preheated with exhaust heat from furnace gases before it is routed to a desulphurization bed operating at 365 °C, after which steam at intermediate pressure from the back-pressure steam turbine is added, with a resulting S/C ratio of 2.83 in the base case. It is further heated with the exhaust air to a temperature of 500 °C before entering the pre-reformer bed, where all higher hydrocarbons are converted. After further pre-heating to 747 °C, the fuel/steam mixture is fed to the reformer tubes, packed with a nickel catalyst. The reactor effluent leaves at 890 °C and 32 bar under equilibrium conditions, achieving a methane conversion of approximately 83 %. The heat for the reforming reactions is provided by combustion in the furnace using preheated air delivered by a blower and the PSA off-gas with a small portion of the PSA inlet feed. Air is supplied with 10 % excess relative to stoichiometric requirements to ensure full fuel conversion. In the plant design presented in this work, only sufficient steam is raised to satisfy the S/C specification, while the low-pressure (LP) steam required for amine solvent regeneration is generated entirely in a dedicated boiler after the WGS section. By doing so, the resulting hydrogen efficiency is substantially higher relative to previous studies, at the cost of a decreased power generation in the steam turbine. This results from avoiding the heat losses associated to high pressure (HP) steam generation with the furnace gases, which can be used more effectively to further preheat the feed streams to the reformer, as reflected in prior studies [20].

The hot syngas from the primary reformer is first cooled down by producing HP steam at 94 bar and 410 °C, which is delivered to a backpressure steam turbine to produce some electricity for the plant and to lower the pressure of the steam to the natural gas line before mixing. The cooled syngas stream at 350 °C is fed to a high temperature shift (HTS) adiabatic reactor, after which it is cooled to 220 °C and sent to the low temperature shift (LTS), achieving an overall carbon monoxide (CO) conversion of around 96 %. The shifted syngas is cooled to 125 °C by economizing water fed to the evaporator and generating LP steam for

the amine stripper and is finally cooled to ambient temperature in a heat rejection exchanger. The syngas after water knock out is routed to the MDEA absorption unit where 95 % of the CO_2 is removed. The CO_2 stream obtained from the stripper tops is dehydrated and compressed in four intercooled stages to supercritical pressure, and then further pumped to 110 bar. Therefore, emissions arise from CO_2 slip in the absorption unit, unconverted CH_4 from the reformer and unconverted CO from the WGS shift train, which ultimately results in an overall CO_2 capture of approximately 78 %. The H_2 rich syngas from the absorption tops is fed to the pressure swing adsorption (PSA) unit, modelled with a simplified recovery correlation [21]. As described earlier, the low pressure off-gas and a small portion of the PSA feed are routed to the furnace where they are combusted with air in the burners to provide heat to the reforming reactions. The purified H_2 stream from the PSA is compressed to 60 bar and constitutes the final product.

The focus of this study is to evaluate various energy and CO_2 capture enhancement strategies from a techno-economic perspective based on this underlying process topology. The economic potential of each scheme based on the underlying market scenario is assessed. The identified configurations are succinctly presented in the following section.

2.2. Case description

Five cases will be considered in the present study as summarized in Fig. 2. Detailed process flow diagrams with corresponding stream summaries as well as process modelling assumptions of several units are available in the Supplementary Information. All cases feature the conventional basic layout for pre-combustion CO_2 capture from SMR hydrogen production plant described in the preceding section. The distinctions between the five cases are outlined below:

1. Base case. The conventional layout is followed as outlined above. Fuel for the reformer is mainly sourced from the PSA off-gas, but a small amount of additional fuel is directly split from the CO_2-lean syngas before the PSA to satisfy the reformer heat demand.
2. Advanced heat integration. This case is similar to the base case, with the main difference being better low-temperature heat recovery from the syngas and flue gas streams via parallel heat exchangers. The largest gain comes from recovering a large fraction of the condensation enthalpy in the remaining steam after the water–gas shift unit, aided by a two-phase heat exchanger fed with natural gas and liquid water [22] to reduce the amount of steam that must be supplied via the back-pressure turbine.
3. PSA off-gas recycling. High CO_2 capture ratios are achieved by recycling most of the carbon-containing PSA off-gas for mixing with the pre-reformed natural gas before the main reformer, which requires an off-gas compressor to reach reforming pressures. The heating duty required by the fired tubular reformer is then met primarily by the carbon-free hydrogen product to minimize CO_2 emissions in the flue gas from the reformer furnace.
4. Ohmic heating. This case heats the main reformer using electricity instead of fuel combustion, greatly reducing the amount of fuel that needs to be combusted. Thus, most of the PSA off-gas is recycled to the main reformer, yielding a higher CO_2 capture performance while avoiding the costly product hydrogen combustion of the previous case. The fraction of the PSA off-gas that is combusted is used to maximize pre-heating of the natural gas and steam to reduce overall electricity demand in the reformer.
5. Pyrolysis. This final case is identical to case 2 except for displacing the pre-reformer with a molten salt pyrolysis reactor to crack the higher hydrocarbons and remove the resulting pure carbon from the system, thus producing another valuable product and reducing the steam required to achieve a specified degree of reforming. To maximize carbon formation, the IP steam from the steam turbine exhaust is only fed after the pyrolysis reactor. Heat for pyrolysis is supplied with the furnace exhaust gases.

2.3. Plant performance parameters

In this section the performance indicators are defined, attending to their nature. Energy performance efficiency is firstly presented followed by the environmental metrics (CO_2 emissions). Finally, the economic framework, evaluation parameters and key assumptions are outlined.

2.3.1. Energy

H_2 efficiency (η_{H_2}) as defined in Eq. (1) is the most relevant energetic parameter to be determined for the plant models, as it directly reflects the degree to which the original heating value of the natural gas feed is converted into H_2. Secondly, electrical efficiency shown in Eq. (2) also illustrates the additional power input to the plant that may be required to achieve such conversion. For the pyrolysis case, a carbon production efficiency is defined in a similar manner in Eq. (3). Hydrogen, carbon, and electricity are weighted equally in the net efficiency 1 calculation (η_1) in Eq. (4), while in the net efficiency 2 definition (η_2), electricity is subtracted from the natural gas heat input, under the sign convention that power imports have a negative value, as reflected in Eq. (5). This second definition is relevant to the electrically heated reformer case where clean electricity is weighted equally to natural gas and the associated costs to capture, transport, and store the produced CO_2.

$$\eta_{H_2} = \frac{\dot{m}_{H_2} LHV_{H_2}}{\dot{m}_{NG} LHV_{NG}} \tag{1}$$

$$\eta_{El} = \frac{\dot{W}_{net}}{\dot{m}_{NG} LHV_{NG}} \tag{2}$$

$$\eta_{C} = \frac{\dot{m}_{C} LHV_{C}}{\dot{m}_{NG} LHV_{NG}} \tag{3}$$

$$\eta_1 = \frac{\dot{m}_{H_2} LHV_{H_2} + \dot{W}_{net} + \dot{m}_{C} LHV_{C}}{\dot{m}_{NG} LHV_{NG}} = \eta_{H_2} + \eta_{El} + \eta_{C} \tag{4}$$

$$\eta_2 = \frac{\dot{m}_{H_2} LHV_{H_2} + \dot{m}_{C} LHV_{C}}{\dot{m}_{NG} LHV_{NG} - \dot{W}_{net}} \tag{5}$$

2.3.2. Environmental

Environmental performance is defined based on CO_2 capture ratio (C_{CO_2}) in Eq. (6) and specific emissions (E_{CO_2}) in Eq. (7). For the pyrolysis case, Eq. (6) counts the carbon product as additional CO_2 captured by converting the mass flow rate of carbon to the mass flow rate of CO_2 if it were to be combusted, where M_r is the molar weight.

$$C_{CO_2} = \frac{\dot{m}_{CO_2,cap} + \dot{m}_{C} \frac{M_{r,CO_2}}{M_{r,C}}}{\dot{m}_{CO_2,emit} + \dot{m}_{CO_2,cap} + \dot{m}_{C} \frac{M_{r,CO_2}}{M_{r,C}}} \tag{6}$$

$$E_{CO_2} = \frac{\dot{m}_{CO_2,emit}}{\dot{m}_{H_2}} \tag{7}$$

CO_2 emissions have a direct effect on economic performance when a CO_2 tax is included in the evaluation, as detailed in the following section. Indirect emissions from electricity imports are ignored under the assumption that these plants will be deployed when the power sector has become largely decarbonized and taxation of any remaining CO_2 emissions is included in the electricity price.

2.3.3. Economic

The economic evaluation of the SMR-MDEA plant configurations was carried out in a dedicated tool created by the authors for the standardized economic assessment (SEA) of novel chemical and energy plants [23]. A user's guide is also available for download [24]. The tool allows for convenient determination of the capital cost of the different plant units, using equipment specific correlations from Turton et al. [25] or simplified capacity cost correlations for standard units (Table 1), and scaling these costs for currency, year, and location. In Table 1, the parameters for the

Table 1
Equipment cost scaling parameters used for specialized process units [11].

Unit	Scaling parameter	Cost year	Reference cost (M€)	Reference scale	Scaling exponent
Fired tubular reformer	Heat requirement (MW)	2007	7.77	31.91	0.67
Water-gas shift	Plant fuel input (MW)	2007	9.50	1246.06	0.67
Pre-reformer	Plant fuel input (MW)	2005	17.50	1800.00	0.75
CO_2 capture	CO_2 capture rate (kg/s)	2011	46.14	68.20	0.8
PSA unit	Inlet flowrate (kmol/s)	2007	27.96	4.74	0.67
Desulphurizer	Plant fuel input (MW)	2011	0.66	413.80	0.67

Table 2
Basis assumptions for the economic evaluation.

Location	Western Europe
Cost year	2020
Currency	€

Table 3
Economic evaluation assumptions [17,26].

Capital estimation methodology		
Bare Erected Cost (BEC)		SEA Tool Estimate
Engineering Procurement and Construction (EPC)		10 % of BEC
Project Contingency (PC)		20 % of (BEC + EPC)
Owner's Costs (OC)		15 % of (BEC + EPC + PC)
Total Overnight Costs (TOC)		BEC + EPC + PC + OC
Operating & maintenance costs		
Fixed		
Maintenance	2.5	%TOC
Insurance	1	%TOC
Labour	60	k€/y-p
Operators	20	Persons
Variable		
Electricity	60	€/MWh
Chemicals & catalysts	130	k€/year
Process water	6	€/ton
Make-up water	0.35	€/ton
CO_2 tax	100	€/ton
CO_2 transport and storage	10	€/ton
Carbon sales price *	400	€/ton
Cash flow analysis assumptions		
1st year capacity factor	65	%
Remaining years	85	%
Discount Rate	8	%
Construction period	3	years
Plant Lifetime	25	years

* Implemented as a negative cost in the pyrolysis case.

fired tubular reformer were modified to use the heat requirement for driving the endothermic reaction as a scaling parameter instead of the plant fuel input. This modification reflects the increase in unit cost in the cases with PSA off-gas recycle that increased the reforming load.

Furthermore, the fixed and variable operational costs are estimated to enable the calculation of the levelized cost of hydrogen (LCOH), which is defined as the price of the product that yields a net present value (NPV) of 0 at the end of the plant lifetime. The NPV is calculated through the summations of the annual discounted cash flow rates (ACF_t) over the construction period and operating lifetime (n), as reflected in Eq. (8), where i is the discount rate. The ACF_t is determined in Eq. (9) with the maximum yearly hydrogen production (P_{H_2}), the cash flows of variable (C_{VOM}), fixed (C_{FOM}) operating and maintenance and capital (C_{CAPEX}), where ϕ is the capacity factor of the plant. On the other hand, the CO_2 avoidance cost is determined by comparison to an unabated SMR plant as shown in Eq. (10), considering no CO_2 taxation. In addition, the marginal CO_2 avoidance cost in Eq. (11) is determined as the inverse of the rate at which CO_2 emissions reduce with increased hydrogen production cost. This performance metric is used in cases where different methods of increasing the CO_2 capture rate of the plant (e.g., a higher S/C ratio) are evaluated to quantify the marginal cost of avoiding the next unit of CO_2.

$$NPV = \sum_{t=0}^{n} \frac{ACF_t}{(1+i)^t} \tag{8}$$

$$ACF_t = \phi \cdot (LCOH \cdot P_{H_2} - C_{VOM}) - C_{Capital} - C_{FOM} \tag{9}$$

$$CAC = \frac{LCOH_{CCS} - LCOH_{ref}}{E_{CO_2,ref} - E_{CO_2,CCS}} \tag{10}$$

$$MCAC = -\left(\frac{d(E_{CO_2,CCS})}{d(LCOH_{CCS})}\right)^{-1} \tag{11}$$

To consistently carry out the economic evaluation, it is necessary to define a cost estimation basis (year, currency, and location), as shown in Table 2.

Other relevant economic assumptions used in the capital and operating & maintenance cost estimation methodology of the present study are summarized in Table 3. Detailed SEA tool files for the plants evaluated in this work are available online.[1]

3. Results and discussion

Results will be presented and discussed in five parts: 1) an exploration of the cost of using the S/C ratio to increase the CO_2 capture ratio in the base case SMR-MDEA plant configuration, 2) the effect of advanced heat integration on the plant techno-economic performance, 3) the cost of employing flue gas recirculation to achieve high CO_2 capture ratios, 4) electrical reformer heating for blue-green hydrogen production, and 5) molten salt pyrolysis replacing the pre-reformer for blue-turquoise hydrogen production. Detailed performance figures of the main cases are given in the Appendix.

3.1. The cost of a higher S/C ratio

Only about 85 % of the produced CO_2 is captured in the conventional process configuration (Case 1 in Fig. 2) with a commonly assumed S/C ratio close to 4 [11,13]. Some of the CO_2 emissions originate from the incomplete CO_2 capture in the MDEA unit (here assumed to achieve 95 % CO_2 capture), but most emissions arise from the unconverted CO and CH_4 in the shifted syngas stream. These carbon-containing fuel gases are separated out in the PSA off-gas stream and combusted in the fired tubular reformer (FTR) furnace to supply the reforming heat, leading to significant CO_2 emissions.

The simplest way to reduce these emissions is to increase the S/C ratio, achieving more reforming of CH_4 and shifting of CO to convert a higher fraction of these carbon-containing fuel gases to CO_2 that can be extracted by the MDEA unit. However, Fig. 3a shows that raising additional steam imposes a substantial energy penalty on the plant, increasing the cost of the produced hydrogen. As illustrated in Fig. 3b, the avoided CO_2 taxes from a higher S/C ratio are not sufficient to cancel out the increase in hydrogen production cost (primarily created by the lower hydrogen production efficiency) at the default CO_2 tax of 100 €/ton, although the trade-off becomes relatively close at lower S/C ratios.

Using data of LCOH and specific CO_2 emissions, the marginal amount of CO_2 avoided (in kg) per € of additional hydrogen production cost can be calculated at all points by fitting a curve to the data presented in Fig. 3c and taking its derivative. The inverse of this derivative is the

[1] https://bit.ly/3lViy4r.

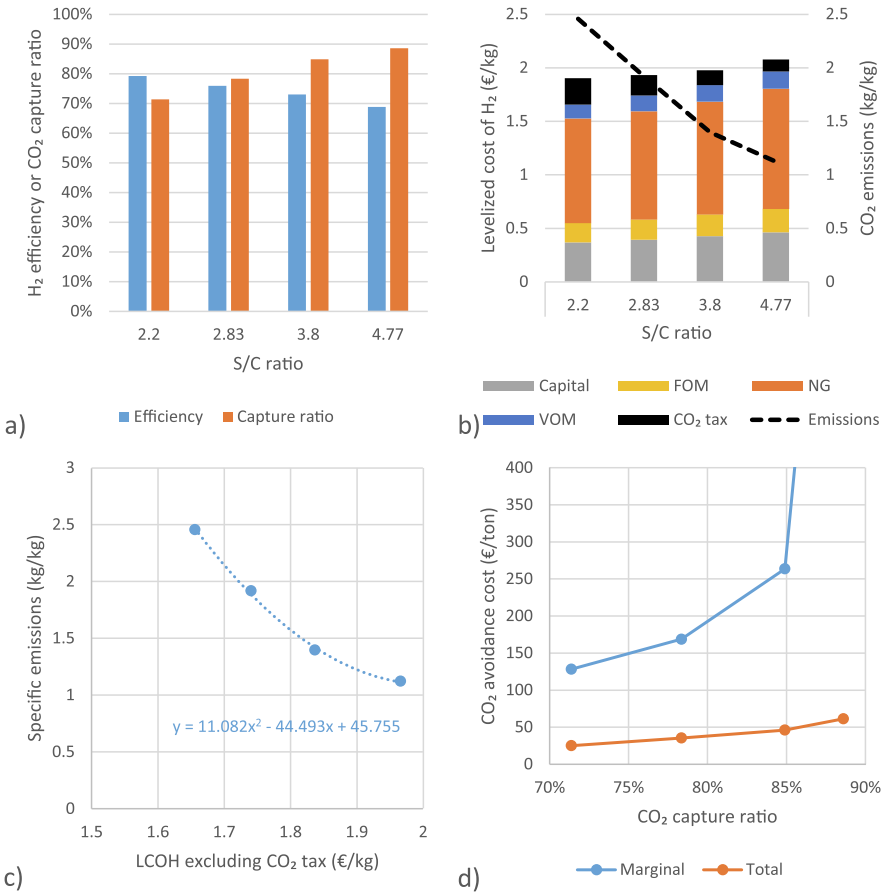

Fig. 3. An illustration of the rising marginal CO_2 avoidance costs from capturing more CO_2 via higher S/C ratios: a) the trade-off between hydrogen production efficiency and CO_2 capture ratio, b) the increase in LCOH with higher S/C ratios, c) the correlation between specific CO_2 emissions and hydrogen production costs, and d) the marginal CO_2 avoidance cost as a function of CO_2 capture ratio.

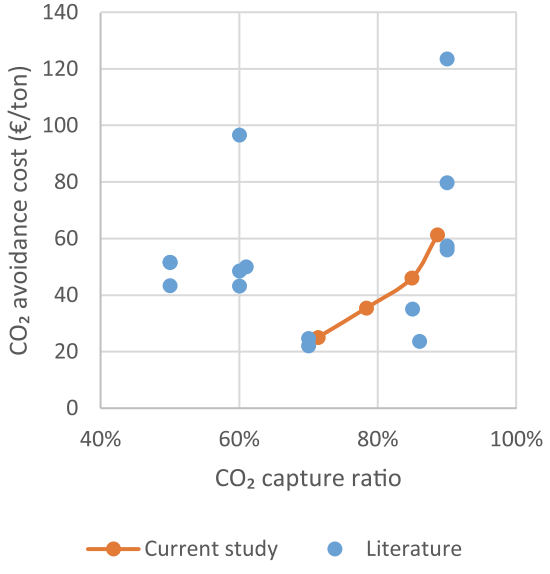

Fig. 4. Comparison of the current simulations to literature values collected by Parkinson et al. [27].

marginal CO_2 avoidance cost involved in avoiding the next unit of CO_2 at any point on the curve (Eq. (11)). As shown in Fig. 3d, this marginal CO_2 avoidance cost rises rapidly when approaching 90 % CO_2 capture. In fact, going beyond 80 % capture already involves a cost that is unlikely to cancel out rising CO_2 taxes in the future. In other words, it will remain optimal to capture less than 80 % of the produced CO_2, even with high future CO_2 taxes (up to 200 €/ton).

Fig. 3d also shows the total CO_2 avoidance cost (Eq. (10)), calculated through comparison to an SMR plant without CO_2 capture that returned a hydrogen production cost of 1.50 €/kg with CO_2 emissions of 8.76 kg CO_2 per kg H_2. The unabated plant was simulated with an S/C ratio of 2.7, following earlier studies [11,13]. As shown, CO_2 avoidance costs can be as low as 25 €/ton for the S/C = 2.2 case, but this is not a reliable reflection because the unabated plant would also benefit from lower S/C ratios, where carbon deposition in the reformer might cause significant technical challenges. The S/C = 2.83 case is close to the S/C ratio of 2.7 used in the unabated plant and returns CO_2 avoidance costs of 35.5 €/ton. Thus, almost 80 % of CO_2 can be captured at an attractively low cost by keeping the S/C ratio of an SMR plant constant and simply adding the MDEA unit (with CO_2 compression) before the PSA. This low cost is enabled by the low steam requirement of the MDEA process, which can be supplied at almost no extra cost from excess low-grade heat available after the WGS reactors. However, the very high marginal CO_2 avoidance cost of increasing the S/C ratio to achieve higher CO_2 capture ratios increases the total CO_2 avoidance cost considerably. For example, the total CO_2 avoidance cost of the S/C = 4.77 case rises by 73 % to 61.3 €/ton even though it only captures 13 % more CO_2 than the S/C = 2.83 case.

The incomplete CO_2 capture from these plants imposes significant costs from CO_2 taxation, as illustrated by the black bars in Fig. 3b. There

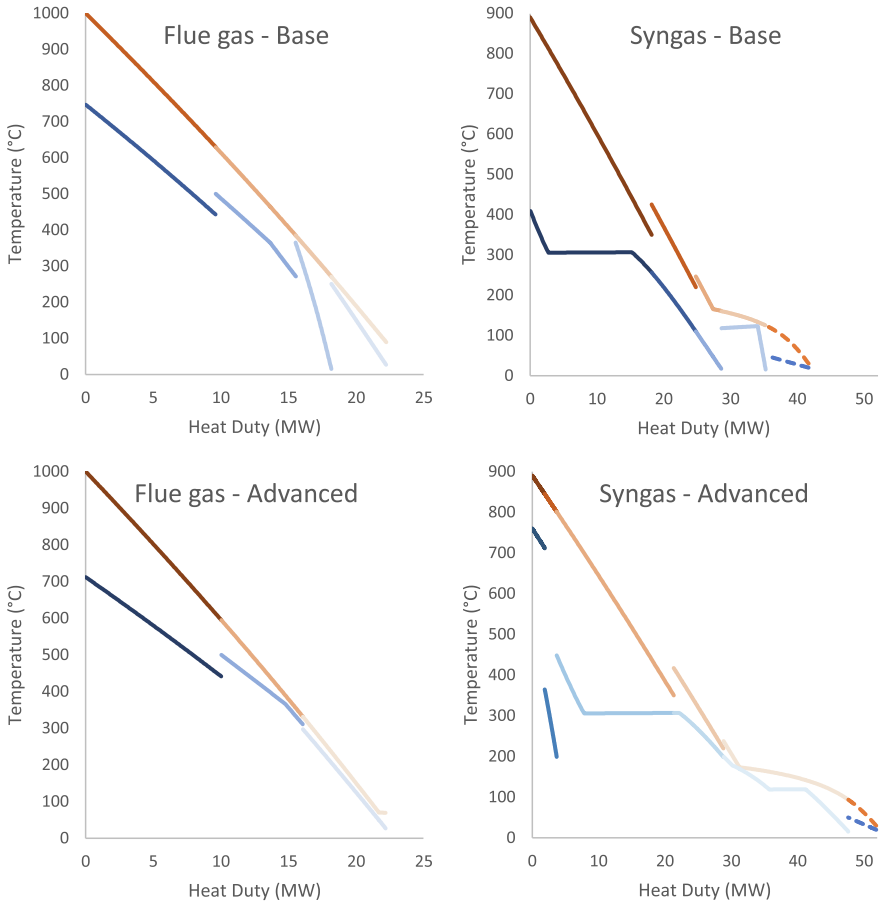

Fig. 5. Heat exchange duty diagrams for the hot combustor flue gas (left) and syngas (right) process streams in the conventional configuration (top) and the advanced heat integration (bottom). Different colour shades are used to differentiate individual heat exchangers, where dashed lines indicate heat rejection.

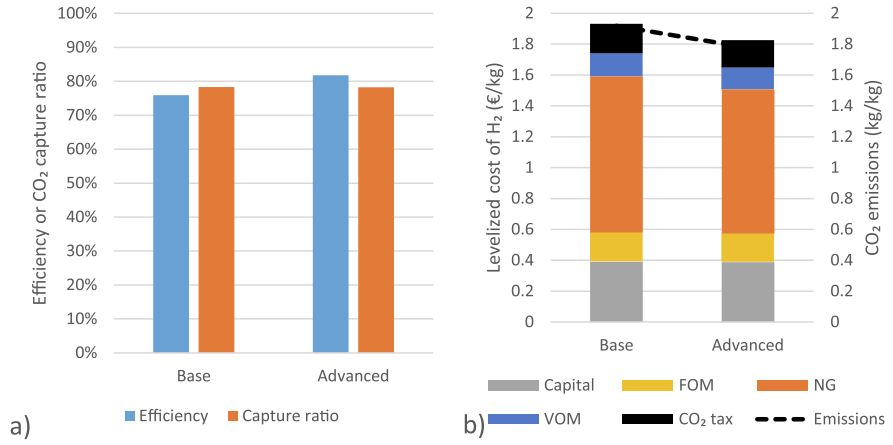

Fig. 6. The effect of advanced heat integration on efficiency and CO_2 capture ratio (a) and hydrogen production cost (b).

should be some scope for plants to adjust their S/C ratios dynamically in response to uncertain developments in the CO_2 price over future decades, but extreme CO_2 taxation will be needed to justify commonly assumed S/C ratios of 4. In fact, the lowest S/C ratio of 2.2 remains the most economical even though it captures only 71 % of CO_2. However, since carbon deposition might render this case impractical, the case with an S/C ratio of 2.83 (achieving almost 80 % CO_2 capture) is selected for the remainder of the study.

Finally, the economic performance of the conventional CO_2 capture configuration analysed in Fig. 3 is compared to a range of literature studies in Fig. 4. In general, the cases with a low CO_2 capture ratio involve pre-combustion CO_2 capture without a higher S/C ratio or the inclusion of a low-temperature water–gas shift step to maximize CO_2 production before the MDEA unit. Cases achieving 90 % capture, on the other hand, involve post-combustion CO_2 capture from the FTR furnace flue gas. Although there is substantial scatter in the literature data due to different CO_2 capture configurations, heat integration networks, and economic assumptions, results from the present study fall toward the centre of the

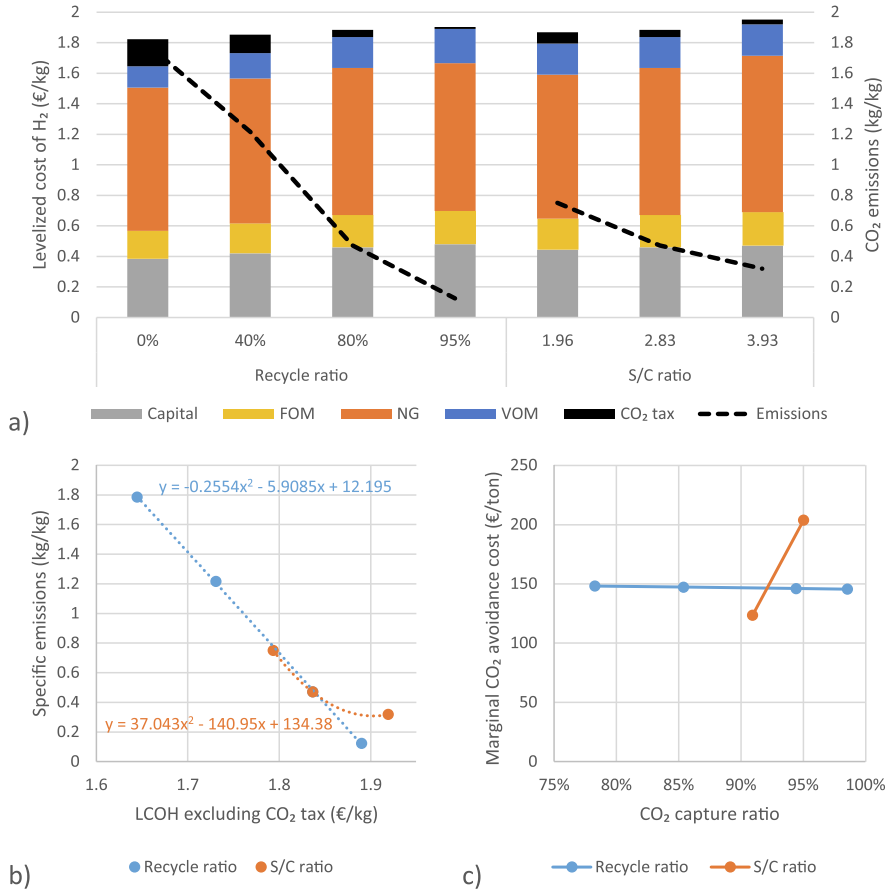

Fig. 7. The cost of avoiding more CO_2 using PSA off-gas recirculation: a) the increase in LCOH with increased CO_2 capture, b) the correlation between specific CO_2 emissions and hydrogen production costs, and c) the marginal CO_2 avoidance cost as a function of CO_2 capture ratio. The cases varying the recycle ratio use a S/C ratio of 2.83, whereas the cases varying the S/C ratio use a recycle ratio of 80%.

range. The penalty of additional steam production and exothermic low-temperature water–gas shift used to achieve a high CO_2 capture ratio in this work appears to be similar to that of post-combustion CO_2 capture used to achieve 90 % CO_2 capture in literature [17,28].

3.2. Advanced heat integration

There is considerable potential to increase the efficiency of the plant by recovering more of the heat from the two main process streams: 1) using the flue gas to preheat fuel for the FTR furnace in parallel to the air and 2) recovering more of the condensation enthalpy in the WGS outlet gas by employing a parallel heat exchanger including a two-phase heat exchanger with an inlet of mixed natural gas and water to produce more process steam at low temperatures. These two parallel-flow heat exchangers were included in the heat exchange network and sized to respect a minimum approach temperature of 5 °C.

The heat exchanger duty diagrams are shown in Fig. 5, illustrating how these measures recovered more heat from both FTR outlet streams. In total, heat recovery increases by 12.3 MW (9.5 % of LHV input) when advanced heat integration is employed. Heat recovery from the combustor flue gas is about the same in both cases because the improved heat recovery from fuel pre-heating is cancelled out by the smaller flue gas stream resulting from the lower reformer heat demand (which, in turn, results from greater fuel pre-heating, as discussed in the next paragraph). On the other hand, heat recovery from the syngas stream is strongly increased by the advanced heat integration, mainly due to the greater latent heat recovery and, to a lesser degree, due to lower temperatures in the WGS reactors that increase conversion and heat release from the exothermic reaction.

Fig. 6 illustrates the effect of these improvements. Hydrogen production efficiency improves by fully 5.9 %-points with advanced heat recovery. Since the advanced heat integration case facilitated more of the steam to be raised from heat that is rejected in the base case, more of the high-grade heat could instead be used to pre-heat the natural gas and steam mixture to the reformer in a high-temperature heat exchanger made from Ni-alloy. This created a smaller reformer heat duty, reducing the need for syngas combustion and allowing more of the fuel heating value to be extracted as hydrogen in the PSA.

The most important cost saving in Fig. 6b is the lower natural gas cost resulting from the reduced fuel consumption per unit hydrogen produced. Variable operating costs and CO_2 taxes drop by a similar amount as these costs can be levelized over a larger quantity of produced hydrogen. However, levelized capital costs and fixed O&M costs (assumed proportional to capital costs) remain almost unchanged because of the more expensive heat exchange network in the case with advanced heat integration. Several heat exchangers have closer approaches in this configuration, requiring larger heat exchange surface areas and higher capital costs, cancelling out the benefit of levelizing the capital cost over a larger hydrogen output. In addition, a 50 % contingency is added to the cost of the parallel heat exchanger extracting maximum duty from the condensing steam in the syngas stream, given that it will be more technically challenging to construct.

Due to the promising performance of the SMR plant with advanced heat integration, this configuration will be studied as the base case for the remainder of the cases in this work.

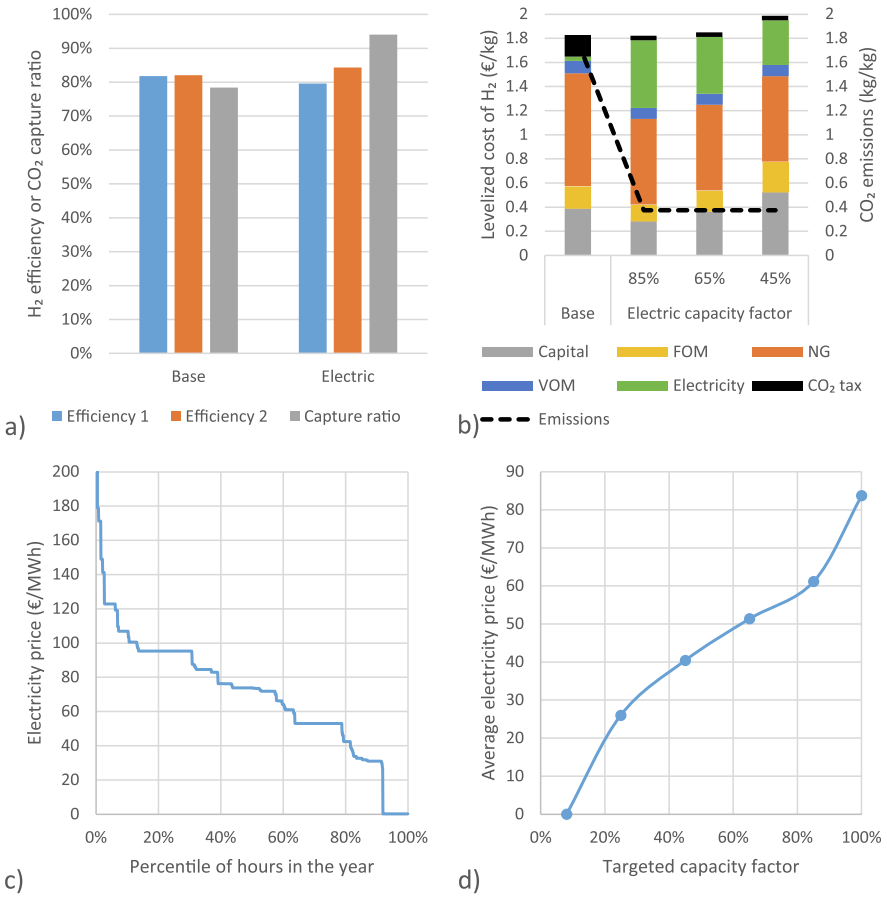

Fig. 8. The effect of using ohmic heating in the reformer. In panel a, Efficiency 1 is given by Eq. (4) and Efficiency 2 by Eq. (5). Three different trade-offs between electricity price and capacity factor are investigated for hydrogen production costs in panel b, using a simulated electricity price duration curve (panels c & d) for a highly decarbonized future energy system [30]. The base case refers to the configuration with advanced heat integration without flue gas recirculation.

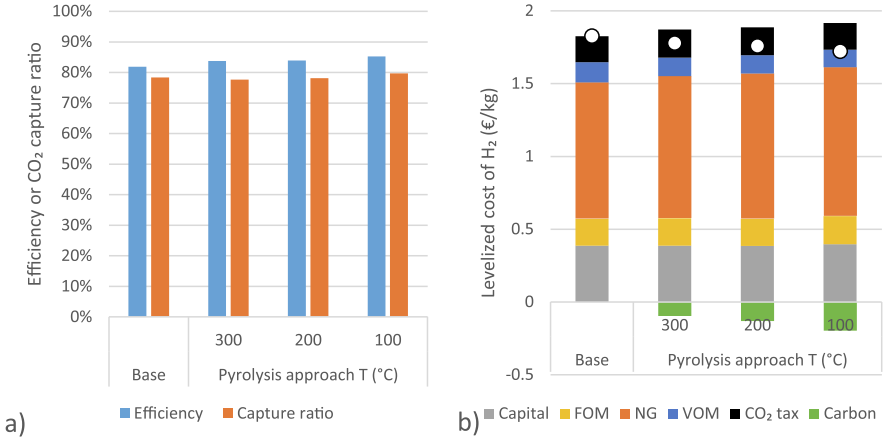

Fig. 9. The effect of replacing the pre-reformer with a molten salt pyrolysis reactor. Three different pyrolysis reactor approach temperatures (below the reactor temperature of 700 °C) are investigated. In panel b, the white dots indicate the net levelized cost of hydrogen after carbon sales at a price of 400 €/ton. The S/C ratio was kept constant at 2.83. The base case refers to the configuration with advanced heat integration without flue gas recirculation.

3.3. *Off-gas recirculation for high CO_2 capture ratios*

A key weakness of the conventional SMR-MDEA configuration is the relatively low CO_2 capture ratio achieved. This drawback can be overcome via off-gas recirculation as illustrated in Fig. 2 (Case 3), where most of the carbon-containing fuel gases in the PSA off-gas are recycled to the reformer, replaced by pure hydrogen from the PSA for combustion. The effects of this configuration are illustrated in Fig. 7, exploring two ways of exchanging CO_2 capture for efficiency: 1) the recycle ratio and 2) the S/C ratio.

Fig. 7a shows that, at the default CO_2 tax of 100 €/ton, reductions in CO_2 taxes almost cancel out increases in hydrogen production costs as the recycle ratio is increased. Higher recycle ratios increase the hydrogen production cost mainly due to increasing capital costs and

electricity consumption from the recycle compressor and the increased equipment sizes caused by a larger recycled gas volume. Hydrogen production efficiency is virtually unaffected by more recycling, keeping natural gas costs almost constant.

Increasing the S/C ratio at an already high recycle ratio of 80 % has a reasonable cost up to 95 % capture at an S/C ratio of 2.83, but further CO_2 reductions up to an S/C ratio of 3.93 are very costly. This is illustrated by Fig. 7c where the sharp increase in marginal CO_2 avoidance cost with CO_2 capture ratio for the S/C ratio line is shown. The third point at a S/C ratio of 3.93 is not shown on Fig. 7c because it returns a negative number as the second order polynomial trendline in Fig. 7b is just starting to trend upwards at the rightmost S/C ratio data point. Nonetheless, the data clearly shows that marginal CO_2 avoidance costs beyond 95 % capture become excessive when the S/C ratio is used to increase CO_2 avoidance in a situation with 80 % PSA off-gas recycling.

On the other hand, Fig. 7c shows a constant marginal CO_2 avoidance cost around 150 €/ton for increasing the CO_2 capture ratio via PSA off-gas recycling at a constant S/C ratio. In other words, a CO_2 price above 150 €/ton would flip the optimal configuration from one with no recycle and less than 80 % CO_2 capture to one with the maximum practical recycle ratio capturing close to 100 % of the produced CO_2. It is noted that impurities (mainly N_2) in the natural gas will constrain this strategy below 100 % CO_2 capture. The natural gas considered in the present study contains 0.89 % N_2, and this component fraction in the PSA off-gas increases from 1.2 % in the case without recycling to 15.7 % when 95 % of the off gas is recycled. This level of N_2 accumulation is not yet problematic, but natural gases containing more N_2 may create excessive accumulation in the recycle loop when very high CO_2 capture ratios are desired, increasing the required size of the process units and the power consumption of the recycle compressor.

Even though this strategy appears to be a viable pathway to high CO_2 capture ratios, the marginal cost of 150 €/ton needed to avoid the last 20 % of CO_2 will most likely be higher than that achievable from conventional post-combustion CO_2 capture after the FTR furnace. In the case with 0 % recycle in Fig. 7, the flue gas contains 6 % CO_2 (about 8 % when the flue gas is dried), which is considerably more than flue gas from a natural gas-fired power plant. Thus, post-combustion capture should cost about 70 €/ton in this case based on the review of Rubin et al. [29], which is considerably lower than the 150 €/ton achieved via PSA off-gas recycling. Avoiding the first 78 % of CO_2 at 35 €/ton using pre-combustion capture and an additional 20 % at 70 €/ton using post-combustion capture (which can be retrofitted when needed) therefore appears to be an attractive strategy.

3.4. Ohmic reformer heating for blue-green hydrogen

Given the rising interest in green hydrogen production from electricity, the blue-green process configuration (Case 4 in Fig. 2) is proposed where the endothermic reforming reaction is driven by electrical instead of combustion heat. In most cases, the electrical energy used for this purpose would be much more expensive than the low-grade PSA off-gas fuel used for combustion, but there are significant advantages related to an electrified reformer to counterbalance this drawback.

First, the reformer can be operated at higher temperatures to achieve greater methane conversion at a given S/C ratio. With electrical heating, FTR reformer tubes are no longer needed, removing the structural constraint of tube construction materials becoming too weak to carry the pressure load at elevated temperatures. Instead, the catalyst can be housed in a single pressurized vessel (supported by an external pressure shell) with electrical heating rods inserted. Second, despite the higher temperatures, this simplified reformer is expected to be considerably cheaper than the conventional FTR furnace with many reformer tubes. In the present work, a 50 % cost reduction is assumed, which is a rough assumption justified by its low impact on the results (the LCOH varies by only by ± 1 % if the electric reformer cost is varied between 25 % and 75 % of the regular reformer cost.

Fig. 8 shows the comparison of blue-green hydrogen production to the conventional blue configuration. As electricity makes up almost a quarter of the input energy, it accounts for a substantial portion of the LCOH. Thus, it may be interesting to operate the plant primarily when electricity prices are lower at the cost of a lower capacity factor (which leads to higher levelized costs for capital and fixed O&M). This trade-off is investigated using simulated electricity prices for a future near-zero carbon electricity system coupled between Norway and Germany [30]. However, such a decarbonized electricity system based largely on wind and solar power is a long-term prospect. In the near-term, low-carbon hydrogen production via electrified reforming is a realistic option only in regions where hydropower dominates the electricity mix (e.g., Norway).

Fig. 8c shows the simulated electricity prices for one year arranged from highest to lowest [30]. Ideally, the blue-green hydrogen plant would ramp down during the most expensive hours and only operate during cheaper hours. The positive effect of this operating strategy on average annual electricity prices for the plant is shown in Fig. 8d. However, it is noted that this is an idealized assumption because 1) there will be technical constraints to the degree to which the plant can ramp to follow electricity prices, 2) the electricity price curve in Fig. 8c will not be known in advance, and 3) hydrogen prices will vary in a real market, becoming increasingly correlated with electricity prices when more green hydrogen is produced.

Even so, the results serve to illustrate that blue-green hydrogen production has economic potential. As shown in Fig. 8a, it achieves much higher CO_2 capture than the pure blue case because much less fuel needs to be combusted, allowing more than half of the PSA off-gas to be recycled. The penalty associated with recycling is also lower compared to the configuration considered in the previous section because the higher reformer temperature facilitates more methane conversion, allowing for more CO_2 production in the WGS reactors that can be captured by the MDEA unit and removed from the recycle loop.

Efficiency is expressed in two ways in Fig. 8a. Efficiency 1 (Eq. (4)) subtracts electricity input from hydrogen LHV output before dividing by natural gas LHV input. Efficiency 2 (Eq. (5)) divides hydrogen LHV output by the sum of natural gas and electricity input. In other words, Efficiency 1 values electricity similar to hydrogen, whereas Efficiency 2 values it similar to natural gas (plus CO_2-related costs). Fig. 8a shows that the blue-green plant achieves similar efficiencies to the base configuration despite its much higher CO_2 capture ratio.

The economic comparison is presented in Fig. 8b. At the default capacity factor of 85 %, LCOH is identical between the blue and blue-green plants. The blue-green configuration makes up for the high electricity costs with reductions in all other cost categories. First, some of the natural gas fuel is replaced by electricity, reducing natural gas costs. However, the combined energy cost of the blue-green plant remains 33 % higher than the blue plant due to the high cost of electrical energy. Capital and fixed O&M costs are also substantially lower in the blue-green plant. Total capital costs of the two plants are similar, but the blue-green plant produces 31.5 % more hydrogen from the same natural gas input, resulting in considerably lower costs on a levelized basis. Capital cost savings per unit hydrogen production originate mainly from the cheaper reformer, simpler heat exchange network, and some economies of scale for the CO_2 capture and PSA units that separate larger amounts of CO_2 and H_2. Finally, the high CO_2 capture ratio of the blue-green plant minimizes costs from CO_2 taxation.

Fig. 8b also shows that the trade of lower electricity prices for higher capital and fixed O&M costs at lower capacity factors is not favourable. Electricity costs are a substantial portion of the LCOH, but not as large as for pure green H_2 from electrolysis that uses electricity for the entire energy supply. Thus, this blue-green plant derives smaller benefits from load-following operation than the pure green alternative. Its role in the future energy system would therefore be more focussed on ramping down in a relatively small fraction of annual hours when electricity is scare (and very expensive), while green hydrogen would concentrate most production into a relatively low number of hours when wind and

solar electricity is available in excess (and very cheap).

3.5. Molten salt pyrolysis for blue-turquoise hydrogen

Hydrogen production from methane pyrolysis, often referred to as turquoise hydrogen, has enjoyed increasing attention in recent years, partly because it produces CO_2-free hydrogen without having to deal with CO_2 transport and storage. However, it is limited by the market for the produced high-purity carbon, which is orders of magnitude smaller than the projected future market for clean hydrogen [31]. Case 5 in Fig. 2 seeks to exploit potential economic benefits of methane pyrolysis while greatly increasing the produced H_2/C ratio to reduce the limitation imposed by the size of the carbon market.

Fig. 9 shows the effect of including pyrolysis on the technical and economic performance of the plant. Since the performance of the pyrolysis reactor under the proposed conditions is highly uncertain at present, cases were specified to achieve equilibrium at different approaches to the reactor temperature of 700 °C. As the pyrolysis reactor is used to replace the pre-reformer in the proposed blue-turquoise SMR configuration, cracking of the higher hydrocarbons is the primary objective. Complete higher hydrocarbon conversion is achieved even at the widest temperature approach of 300 °C (implying equilibrium conditions corresponding to 400 °C), with narrower temperature approaches achieving more methane cracking. Experimental work is required to reveal the degree to which this low level of hydrocarbon cracking can be achieved in a moderately sized reactor, here assumed to be about 10 m tall and 3.3 m in diameter, resulting in a low superficial gas velocity of 0.05 m/s.

Regarding the technical performance, Fig. 9a shows that the CO_2 capture ratio remains unchanged, while a modest efficiency boost is achieved in the pyrolysis configurations. This gain stems from the removal of carbon before the main reformer, which reduces the steam requirement for reaching the specified S/C ratio as well as the amount of CO_2 that needs to be captured and compressed. The produced C/H_2 ratio (in terms of LHV output) varies from 0.06 to 0.13 when the equilibrium approach temperature is varied between 300 and 100 °C. This is about an order of magnitude lower than full natural gas pyrolysis, implying an order of magnitude greater hydrogen production potential at a given carbon market size.

Fig. 9b shows a significant economic benefit to including pyrolysis in the SMR process. Relative to the conventional process, levelized costs of H_2 drop by 2.6–5.7 %, depending on the approach temperature assumed. This cost reduction is achieved even at the relatively low assumed carbon price of 400 €/ton, which is equivalent (in LHV terms) to a hydrogen price of 1.47 €/kg. If high-purity carbon from the pyrolysis process can be sold for 800 €/ton instead, the LCOH reduction relative to the base case increases to 7.7–16.3 %. Savings originate from the increased process efficiency mentioned previously as well as a reduction in capital costs stemming from a smaller reformer, CO_2 capture and compression assembly, and PSA unit (levelized capital costs per unit H_2 stay constant in Fig. 9b because some hydrogen production is displaced by carbon).

These results indicate that pyrolysis technology has the potential to improve the competitiveness of blue hydrogen production from SMR. Experimental studies are needed to reveal the technical feasibility of this approach. However, the low degree of cracking required in the proposed process configuration (mainly higher hydrocarbons) should significantly reduce technical challenges relative to full natural gas pyrolysis. Furthermore, it should be relatively simple to retrofit existing SMR-MDEA plants with pyrolysis pre-treatment to improve profitability when the technology becomes available.

4. Conclusions

An SMR plant equipped with pre-combustion CO_2 capture can achieve 78 % CO_2 avoidance at a relatively low cost of 35 €/ton, but avoiding the remaining 22 % becomes considerably more expensive. While preserving the pre-combustion configuration, higher CO_2 capture ratios can be achieved by increasing the steam-to-carbon ratio or by recycling some PSA off-gas to the reformer, but both methods returned marginal CO_2 avoidance costs of 150 €/ton or above. Thus, applying post-combustion CO_2 capture to the last 22 % of CO_2 will be a more cost-effective solution to achieving very high CO_2 capture ratios from SMR plants.

The economics of pre-combustion CO_2 capture can be further improved in other ways, three of which were investigated in the present study. First, advanced heat integration to recover the condensation enthalpy from excess steam remaining after the water–gas shift step can reduce hydrogen production costs by about 6 % through increased hydrogen production efficiency. Second, electrically heated reforming for blue-green hydrogen production, a simplified process configuration that inherently achieves high CO_2 avoidance, offers a competitive solution if a reliable supply of carbon-free electricity is available below 60 €/MWh. This configuration could also provide grid services by ramping down when electricity is scarce and prices are excessively high. Third, the use of molten salt pyrolysis instead of conventional pre-reforming for blue-turquoise hydrogen production can reduce hydrogen production costs by approximately 10 %, depending on the selling price of the pure carbon by-product.

Thus, SMR with pre-combustion capture presents a versatile solution for near-term low-carbon hydrogen production. In regions with modest CO_2 prices, plants capturing less than 80 % of CO_2 at moderate costs offer an attractive solution with the safeguard of adding post-combustion retrofits to capture the remaining 20 % when CO_2 prices rise in the future. As low-carbon electricity capacity expands, the possibility of electrified reforming will become increasingly attractive in regions with excellent renewable energy resources. Furthermore, additional gains are possible via advanced heat integration strategies and molten salt pyrolysis replacing pre-reformers in the future. Such versatility and improvements will keep SMR competitive against emerging solutions for many years to come as the role of hydrogen in global decarbonization continues to expand.

CRediT authorship contribution statement

Florian Pruvost: Investigation, Software, Visualization, Formal analysis, Writing – original draft. **Schalk Cloete:** Conceptualization, Methodology, Supervision, Formal analysis, Writing – original draft, Writing – review & editing. **Carlos Arnaiz del Pozo:** Supervision, Investigation, Writing – original draft. **Abdelghafour Zaabout:** Funding acquisition, Project administration, Resources.

Declaration of Competing Interest

The authors declare that they have no known competing financial interests or personal relationships that could have appeared to influence the work reported in this paper.

Data availability

Data will be made available on request.

Acknowledgement

The authors gratefully acknowledge the financial support of the Research Council of Norway under the FRINATEK program (project number: 302819).

Appendix

A more detailed breakdown of the technical performance of the main cases considered is provided in Table 4. Full details for each case are available in the individual techno-economic assessment files shared online.[2]

[2] https://bit.ly/3lViy4r.

Table 4
Techno-economic performance metrics of the five main plant configurations and the reference case without CO_2 capture.

Parameter	Unabated	Base case	Advanced	Recycle	Electric	Pyrolysis
Energy						
Natural gas input (kg/s)	2.78	2.78	2.78	2.78	2.78	2.78
Hydrogen production (kg/s)	0.84	0.83	0.90	0.87	1.18	0.84
Carbon production (kg/s)						0.27
Electricity consumption (MW)	0.00	−1.79	−1.95	−4.01	−38.95	−1.66
Hydrogen efficiency (%)	78.19	77.30	83.31	81.05	109.73	78.28
Carbon efficiency (%)	0.00	0.00	0.00	0.00	0.00	6.86
Electric efficiency (%)	0.00	−1.38	−1.51	−3.11	−30.15	−1.29
Efficiency 1 (%) Eq. (4)	78.19	75.92	81.80	77.94	79.58	83.85
Efficiency 2 (%) Eq. (5)	78.19	76.25	82.07	78.61	84.31	84.06
Environmental						
CO_2 capture ratio (%)	0.00	78.34	78.27	94.43	93.99	78.04
Specific CO_2 emissions ($kgCO_2/kgH_2$)	8.76	1.92	1.79	0.47	0.38	1.92
Economic						
Total Overnight cost (M€)	64.83	84.39	89.29	104.02	87.06	84.18
Levelized cost of hydrogen (€/kg)	2.37	1.93	1.82	1.88	1.82	1.76
Capital	0.31	0.39	0.38	0.46	0.28	0.39
Fixed O&M	0.16	0.19	0.18	0.21	0.14	0.19
Natural gas	1.00	1.01	0.94	0.96	0.71	1.00
Variable O&M	0.03	0.15	0.14	0.20	0.65	0.12
CO_2 taxes	0.87	0.19	0.18	0.05	0.04	0.19
Carbon						−0.13
CO_2 avoidance cost (€/ton)		35.46	21.18	41.02	34.46	10.17

Appendix A. Supplementary material

Supplementary data to this article can be found online at https://doi.org/10.1016/j.enconman.2022.116458.

References

[1] IEA. The future of hydrogen: seizing today's opportunities. International Energy Agency; 2019.
[2] EU. Hydrogen Roadmap Europe: a sustainable pathway for the European energy transition. European Union; 2019.
[3] US. Road Map to a US Hydrogen Economy: reducing emissions and driving growth across the nation. Fuel Cell & Hydrogen Energy Association; 2019.
[4] Gummer J, et al. Hydrogen in a low-carbon economy. Committee on Climate Change; 2018.
[5] Bruce S, et al. National hydrogen roadmap: pathways to an economically sustainable hydrogen industry in Australia. CSIRO; 2018.
[6] BMWi. The national hydrogen strategy. The Federal Government. 2021. Available from: https://www.bmbf.de/files/bmwi_Nationale%20Wasserstoffstrategie_Eng_s01.pdf.
[7] Cloete S, Ruhnau O, Hirth L. On capital utilization in the hydrogen economy: the quest to minimize idle capacity in renewables-rich energy systems. Int J Hydrogen Energy 2021;46(1):169–88.
[8] Ryden M, Lyngfelt A, Mattisson T. Two novel approaches for hydrogen production; chemical-looping reforming and steam reforming with carbon dioxide capture by chemical-looping combustion. In: 16th World Hydrogen Energy Conference 2006, WHEC 2006, June 13, 2006 - June 16, 2006. Lyon, France: Association Francaise pour l'Hydrogene et les Piles a; 2006.
[9] Spallina V, et al. Chemical looping reforming in packed-bed reactors: modelling, experimental validation and large-scale reactor design. Fuel Process Technol 2017;156:156–70.
[10] Wassie SA, et al. Hydrogen production with integrated CO2 capture in a novel gas switching reforming reactor: proof-of-concept. Int J Hydrogen Energy 2017;42(21):14367–79.
[11] Spallina V, et al. Techno-economic assessment of membrane assisted fluidized bed reactors for pure H2 production with CO2 capture. Energy Convers Manage 2016;120:257–73.
[12] Cloete S, Khan MN, Amini S. Economic assessment of membrane-assisted autothermal reforming for cost effective hydrogen production with CO2 capture. Int J Hydrogen Energy 2019;44(7):3492–510.
[13] Martínez I, et al. Hydrogen production through sorption enhanced steam reforming of natural gas: thermodynamic plant assessment. Int J Hydrogen Energy 2013;38(35):15180–99.
[14] Nazir SM, et al. Pathways to low-cost clean hydrogen production with gas switching reforming. Int J Hydrogen Energy 2020.
[15] IEA. World Energy Outlook. International Energy Agency; 2020.
[16] IRENA. Green hydrogen cost reduction: Scaling up electrolysers to meet the 1.5 °C climate goal. International Renewable Energy Agency: Abu Dhabi; 2020.
[17] Collodi G, Azzaro G, Ferrari N. Techno-economic evaluation of SMR based standalone (merchant) plant with CCS. IEAGHG, editor; 2017.
[18] Wismann ST, et al. Electrified methane reforming: a compact approach to greener industrial hydrogen production. Science 2019;364(6442):756–9.
[19] Romano MC, Chiesa P, Lozza G. Pre-combustion CO2 capture from natural gas power plants, with ATR and MDEA processes. Int J Greenhouse Gas Control 2010;4(5):785–97.
[20] Arnaiz del Pozo C, et al. The potential of gas switching partial oxidation using advanced oxygen carriers for efficient H2 production with inherent CO2 capture. Appl Sci 2021;11(10):4713.
[21] Nazir SM, et al. Efficient hydrogen production with CO2 capture using gas switching reforming. Energy 2019;185:372–85.
[22] Nazir SM, et al. Gas switching reforming (GSR) for power generation with CO2 capture: process efficiency improvement studies. Energy 2019;167:757–65.
[23] Arnaiz del Pozo C, Cloete S, Jiménez Álvaro Á. Standard Economic Assessment (SEA) Tool; 2021. Available from: https://bit.ly/3IXPWC8.
[24] Arnaiz del Pozo C, Cloete S, Jiménez Álvaro Á. SEA Tool User Guide; 2021. Available from: https://bit.ly/3jq9Bkf.
[25] Turton R, et al. Analysis, synthesis and design of chemical processes: Appendix A. Pearson Education; 2008.
[26] Franco F, et al. European best practice guidelines for CO2 capture technologies. In: CESAR project: European Seventh Framework Programme; 2011.
[27] Parkinson B, et al. Levelized cost of CO2 mitigation from hydrogen production routes. Energy Environ Sci 2019;12(1):19–40.
[28] Khojasteh Salkuyeh Y, Saville BA, MacLean HL. Techno-economic analysis and life cycle assessment of hydrogen production from natural gas using current and emerging technologies. Int J Hydrogen Energy 2017;42(30):18894–909.
[29] Rubin ES, Davison JE, Herzog HJ. The cost of CO2 capture and storage. Int J Greenhouse Gas Control 2015;40:378–400.
[30] Cloete S, et al. Blue hydrogen and industrial base products: The future of fossil fuel exporters in a net-zero world. J Cleaner Prod 2022;363:132347.
[31] Keipi T, Tolvanen H, Konttinen J. Economic analysis of hydrogen production by methane thermal decomposition: Comparison to competing technologies. Energy Convers Manage 2018;159:264–73.